parasitologia

MDPI

Article

Restricted Genetic Diversity of *Plasmodium falciparum* and *Plasmodium vivax* During the 2025 Phase of a Malaria Outbreak in the Bay Islands of Honduras

Lesly Chaver [1], Gloria Ardón [2], Amed Matute [2], Dámaris Ortez [2], Mitzi Castro [1], Fernando Pérez [3], Denis Escobar [3], Hugo O. Valdivia [4] and Gustavo Fontecha [3,*]

[1] Laboratorio Nacional de Vigilancia de Malaria, Secretaría de Salud de Honduras, Tegucigalpa 11101, Honduras; leslychaver@yahoo.com (L.C.); jefaturalab2020@gmail.com (M.C.)
[2] Sanitaria de Islas de la Bahía, Secretaría de Salud de Honduras, Roatán 34101, Honduras; manaardon@gmail.com (G.A.); amedmatute1982@gmail.com (A.M.); ortezds_01@hotmail.com (D.O.)
[3] Instituto de Investigaciones en Microbiología, Facultad de Ciencias, Universidad Nacional Autónoma de Honduras, Tegucigalpa 11101, Honduras; fernandperezz14@gmail.com (F.P.); denis.escobar@unah.edu.hn (D.E.)
[4] Department of Parasitology, U.S. Naval Medical Research Unit SOUTH (NAMRU SOUTH), Lima 07001, Peru; hugo.o.valdivia.ln@health.mil
* Correspondence: gustavo.fontecha@unah.edu.hn; Tel.: +504-33935443

Abstract

Honduras is progressing toward malaria elimination as part of the Mesoamerican goal for 2030. As transmission declines, malaria increasingly occurs in focal outbreaks, particularly in geographically confined settings such as islands. Following an increase in cases beginning in 2024, the Bay Islands Department experienced continued outbreak transmission during 2025. This study characterized the genetic diversity and multilocus haplotype patterns of *Plasmodium falciparum* and *P. vivax* lineages circulating during this outbreak. Cases were confirmed by photo-induced electron transfer PCR (PET-PCR). Genetic diversity was assessed by Sanger sequencing of *pfmsp1* for *P. falciparum*, and *pvcsp* and *pvmsp3α* for *P. vivax*; *pfmdr1* was analysed separately as a drug-resistance marker. Diversity indices and multilocus profiles were analysed using DnaSP. Forty-nine samples were analysed: 18 *P. falciparum* and 31 *P. vivax* infections from three municipalities. All *P. falciparum* isolates carried a single *pfmsp1* haplotype of the K1 allelic family. In *P. vivax*, two concordant multilocus haplotypes were detected: A/A predominated, whereas B/B was observed in five samples, mainly early in the outbreak. The outbreak showed marked *P. falciparum* homogeneity and restricted *P. vivax* multilocus diversity, consistent with focal amplification of limited parasite lineages. However, multiple introductions of genetically similar parasites cannot be excluded.

Keywords: Malaria; outbreak; Bay Islands; Honduras; *Plasmodium vivax*; *Plasmodium falciparum*

Check for updates

Academic Editor: Maurizio Francesco Brivio

Received: 29 July 2026
Revised: 14 September 2026
Accepted: 15 September 2026
Published: 17 September 2026

Copyright: © 2026 by the authors. Licensee MDPI, Basel, Switzerland. This article is an open access article distributed under the terms and conditions of the Creative Commons Attribution (CC BY) license.

1. Introduction

Malaria transmission in Honduras has historically been concentrated in the Eastern and North Atlantic regions of the country, particularly in the department of Gracias a Dios [1]. However, in recent years, focal transmission has re-emerged in other regions, including the Bay Islands Department (Islas de la Bahía), an insular Caribbean department with ecological conditions highly receptive to malaria transmission. This epidemiological context is particularly relevant given that countries in Central America and the island of

Hispaniola have committed to eliminating malaria by 2030, in alignment with the World Health Organization's Global Technical Strategy for Malaria 2016–2030 [2] and regional elimination initiatives. Sustained interruption of transmission in focal areas is therefore critical to achieving these regional targets.

Following a marked increase in malaria cases that began in 2024, the Bay Islands Department experienced a malaria outbreak involving both *Plasmodium vivax* and *P. falciparum*, with spatially heterogeneous transmission across the municipalities of José Santos Guardiola (JSG), Roatán, and Guanaja. This geographically confined and heterogeneous pattern raised concerns regarding focal amplification of parasite populations. In insular settings, restricted gene flow and ecological confinement may amplify founder effects, facilitating rapid expansion of a limited number of parasite lineages once transmission is re-established.

In Honduras, progressive reductions in transmission over the past 25 years have been accompanied by a documented contraction in parasite genetic diversity, including evidence of a population bottleneck in *P. falciparum* along the Honduran–Nicaraguan border [3–7]. Such demographic constriction events reduce effective population size and may facilitate the expansion of a limited number of successful lineages when transmission resurges. In low-transmission and pre-elimination settings, apparent increases in case numbers may therefore reflect not only renewed exposure but also the amplification of genetically homogeneous parasite populations derived from a restricted ancestral pool [8,9].

Conventional epidemiological surveillance alone cannot distinguish between multiple independent introductions and sustained local transmission. Molecular markers provide the necessary resolution to assess parasite population structure, quantify genetic diversity, and detect patterns of homogeneity consistent with recent expansion events [10]. Based on prior molecular surveillance experience in Honduras, four targeted loci were selected for this study: *pfmsp1* and *pfmdr1* for *P. falciparum* [5,11–13], and *pvcsp* and *pvmsp3α* for *P. vivax* [5,7,12,13]. The discriminatory capacity of these markers in Honduras differs by locus, and this distinction is made explicit here. Size-based typing of *pfmsp1* block 2 allelic families and repeat typing of *pvcsp* and *pvmsp3α* have previously resolved multiple variants among Honduran isolates, whereas sequence-level variation within *pfmsp1* allelic subfamilies and across *pfmdr1* has consistently been absent in this parasite population. All four loci encode surface antigens or drug-resistance targets and are therefore subject to selection, which limits their value for demographic inference. Accordingly, *pfmdr1* is reported in this study as a drug-resistance result and is not used as evidence of restricted diversity.

Understanding whether the observed epidemiological pattern resulted from multiple introductions or from local expansion of a limited number of parasite genotypes is critical for guiding elimination strategies in insular and highly receptive settings. Therefore, this study aimed to characterize the genetic diversity, multilocus haplotype structure, and temporal dynamics of *P. falciparum* and *P. vivax* lineages circulating during the 2025 phase of the Bay Islands outbreak, in order to assess patterns consistent with local clonal amplification in a geographically confined setting.

2. Materials and Methods

2.1. Study Area and Sample Collection

This study was conducted in the Bay Islands Department of Honduras, including the municipalities of Roatán, JSG, and Guanaja (Figure 1), where a malaria outbreak involving *P. falciparum* and *P. vivax* was reported in 2024 and 2025. After several years of relatively low case numbers, malaria incidence increased markedly in the Bay Islands beginning in 2024, when 184 cases were reported, representing more than a 100% increase compared with 2022 and 2023, years in which 32 cases were recorded annually. The upward trend

continued into 2025, and by epidemiological week 53, a total of 239 confirmed malaria cases had been documented in the department. Of these, 209 cases (87.4%) were caused by *P. vivax* and 30 (12.6%) by *P. falciparum*. Most cases were classified as autochthonous by the national malaria surveillance system; individual travel histories were not collected as part of the present study. The approximate straight-line distance between Roatán municipality and JSG, located on the same island, is 26 km, whereas Guanaja is located approximately 49 km east of JSG and 74 km east of Roatán.

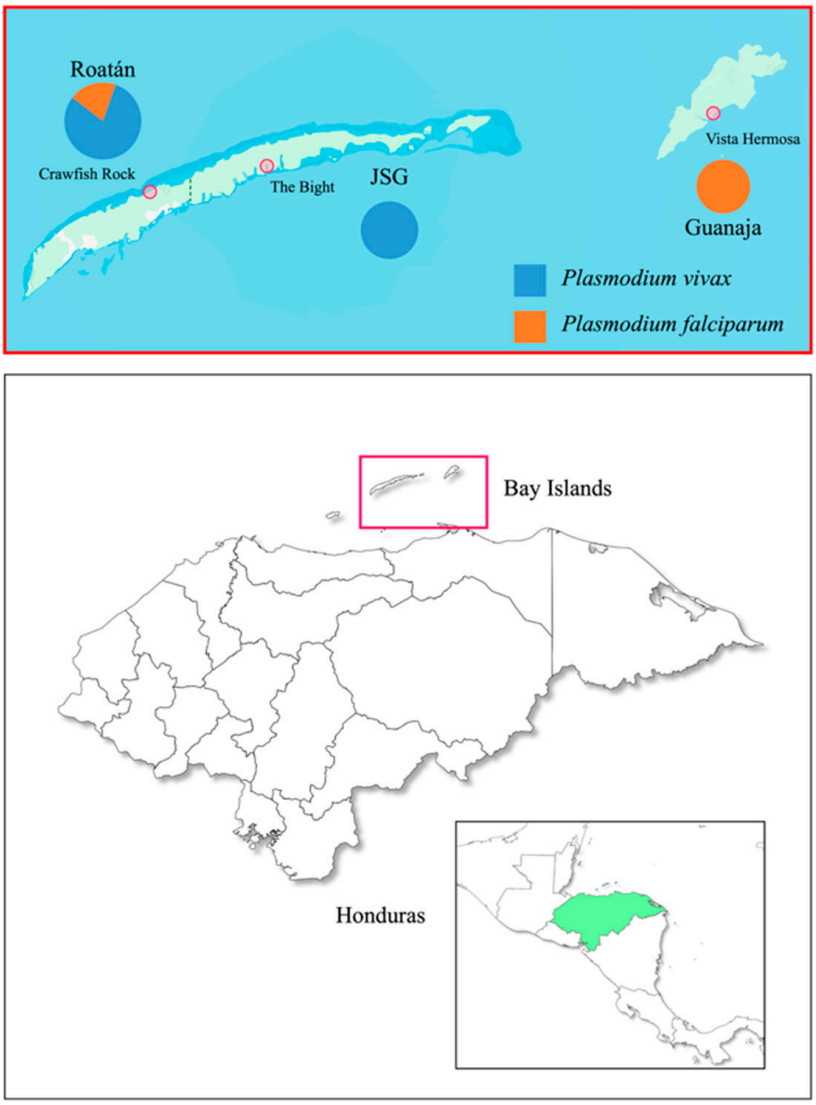


Figure 1. Geographic distribution of malaria-positive samples in the Bay Islands Department, Honduras. Pie charts represent the proportion of *P. vivax* and *P. falciparum* infections by municipality (Roatán, José Santos Guardiola [JSG], and Guanaja), with chart size proportional to the total number of samples analysed per municipality. The highlighted localities indicate the three areas reporting the highest number of cases within each municipality: The Bight (JSG), Crawfish Rock (Roatán), and Vista Hermosa (Guanaja). Insets show the location of the Bay Islands within Honduras, indicated by the red box, and the regional position of Honduras in Central America, highlighted in green. The map of the Bay Islands was obtained from Google Maps (https://www.google.com/maps, accessed on 13 February 2026).

Transmission was spatially heterogeneous across the department. JSG accounted for the largest proportion of reported cases in 2025 (156/239), all attributable to *P. vivax*, with The Bight identified as the main local hotspot. Roatán contributed 61 cases and reported both *P. vivax* and *P. falciparum* infections, with Crawfish Rock among the most

affected localities. Guanaja experienced a distinct focal outbreak of *P. falciparum*, with 22 confirmed cases distributed across four localities, mainly Vista Hermosa, where malaria transmission had not been reported for approximately a decade. The outbreak in Guanaja was first detected in epidemiological week 5 of 2025, when two autochthonous *P. falciparum* cases were identified through passive surveillance. Despite immediate implementation of reactive case detection, indoor residual spraying, supervised treatment, and vector control interventions, additional cases continued to occur through epidemiological week 36, suggesting sustained local transmission. Malaria surveillance in the Bay Islands is conducted through routine passive case detection at health facilities and is complemented during outbreaks by focal response activities such as reactive case detection and vector control interventions.

Of the 239 confirmed malaria cases reported in the Bay Islands Department during 2025, 49 malaria-positive dried blood spot samples collected between January and July 2025 were available through routine surveillance activities and were included in the molecular analysis. The analysed samples represented 20.5% of all confirmed cases and originated from the three affected municipalities: Roatán, JSG, and Guanaja. No additional selection criteria were applied beyond sample availability, so the analysed set constitutes a convenience sample rather than a consecutive or randomly drawn series. Sample identification codes corresponded to the internal routine surveillance numbering system and were not assigned exclusively to the subset analysed in this study. Therefore, gaps in the numerical sequence do not indicate selective exclusion of genotyped malaria-positive samples. The analysed samples constituted a convenience subset of available dried blood spots suitable for molecular analysis, rather than a consecutive series of all cases detected during the study period.

For each analysed sample, a unique sample identification code was assigned, and epidemiological information including the municipality where the case was detected, the date of diagnostic reporting, and the infecting *Plasmodium* species was recorded. Cases were classified as *Plasmodium vivax* (Pv) or *Plasmodium falciparum* (Pf) based on molecular diagnosis. The inclusion of samples spanning multiple municipalities and several months allowed the assessment of spatial and temporal patterns of parasite circulation during the outbreak.

Finger-prick blood samples were obtained from patients with malaria confirmed by thick blood smear microscopy and/or rapid diagnostic tests (RDTs). Blood was spotted onto Whatman® 3MM filter paper (Sigma-Aldrich, Burlington, MA, USA), air-dried, and individually stored in paper envelopes with silica desiccant at room temperature until processing. Epidemiological and basic demographic data, including date of sample collection, municipality of origin, patient age and sex, and *Plasmodium* species diagnosis, were recorded in a project-specific database. Samples were anonymized prior to molecular analysis. Microscopy-based parasite counts were obtained from routine diagnostic records. Asexual parasite density was estimated using the standard formula: number of asexual parasites counted $\times$ 8000/number of leukocytes counted, assuming 8000 leukocytes/μL of blood. For descriptive purposes, parasite densities were categorized as low (<1000 parasites/μL), moderate (1000–9999 parasites/μL), or high ($\geq$10,000 parasites/μL). Gametocyte density was calculated using the same approach based on the number of sexual-stage parasites counted. Parasites were enumerated against 200 leukocytes, extended to 500 leukocytes when few parasites were seen, and counting was stopped once 500 parasites had been recorded; two samples were therefore read against fewer than 200 leukocytes (136 and 93), and the densities derived from those truncated counts should be regarded as approximations. The number of leukocytes counted for each

sample is reported in Supplementary Table S1 so that every density can be recalculated from the raw counts.

Treatment of malaria cases during the outbreak was conducted by the Honduran National Malaria Programme according to national treatment guidelines. *P. vivax* cases received blood-stage treatment together with primaquine for radical cure when not contraindicated. However, detailed individual-level treatment adherence and longitudinal follow-up data were not systematically available for all analysed cases.

2.2. DNA Extraction

Genomic DNA was extracted from dried blood spots using two 2 mm diameter punches per sample. DNA extraction was performed using the Extracta® DNA Prep for PCR kit (QuantaBio, Beverly, MA, USA), following the manufacturer's instructions. Extracted DNA was stored at −20 °C until further molecular analysis.

2.3. Molecular Marker Amplification

Molecular diagnosis of *Plasmodium* infection and species identification were confirmed using photo-induced electron transfer real-time PCR (PET-PCR) [14–16]. All DNA samples were first screened using a genus-specific PET-PCR assay targeting *Plasmodium* spp., and samples testing positive were subsequently analysed with species-specific PET-PCR assays for *P. falciparum* and *P. vivax*. Reactions were run in duplicate using probe-based real-time PCR chemistry, with appropriate positive and no-template controls included in each run. Cycle threshold (Ct) values from the species-specific assays are reported for every sample in Supplementary Table S1 as an indicator of template abundance.

To assess parasite genetic diversity and clonal structure, highly polymorphic molecular markers were selected for each species and amplified using conventional or nested PCR approaches. In *P. falciparum*–positive samples, fragments of the merozoite surface protein 1 (*pfmsp1*) gene were amplified by nested PCR to discriminate the K1, MAD20, and RO33 allelic families [5,17]. In addition, two segments of the multidrug resistance gene 1 (*pfmdr1*) encompassing codons 86, 184, 1034, and 1042 were amplified through nested PCR assays designed to generate fragments suitable for downstream sequencing [11]. The *pfcrt* codon 72–76 region was not genotyped in the present outbreak dataset; therefore, no inference regarding *pfcrt* haplotypes or chloroquine-resistance-associated *pfcrt* variants is made in this study.

For *P. vivax*, genetic diversity was assessed by amplifying fragments of the circumsporozoite protein gene (*pvcsp*) [5] and the merozoite surface protein 3 alpha gene (*pvmsp3α*) [7,18]. The *pvcsp* marker allows discrimination between the major allelic variants VK210 and VK247, which differ in the amino acid repeat motifs within the central repeat region of the gene and are widely used to characterize parasite population structure and geographic distribution.

PCR reactions were performed in a final volume of 50 µL containing template DNA and 10 µM primers (Table 1). Amplification of the *pfmsp1* marker was carried out using KOD DNA polymerase (Sigma-Aldrich, MA, USA) because the laboratory SOP for this nested PCR assay had been optimized and validated using this enzyme. The remaining markers were amplified using Taq DNA polymerase (Promega Corp., Madison, WI, USA) according to the corresponding published protocols and laboratory workflows [5,11–13,19]. All PCR runs included positive control DNA appropriate for the corresponding assay, as well as no-template negative controls to monitor contamination. Control material for *P. falciparum* and *P. vivax* was obtained through the UK NEQAS external quality assessment scheme for parasitology. Each nested *pfmsp1* run additionally included positive control

DNA of the MAD20 and RO33 allelic families alongside the K1 control, so that failure to detect an allelic family could be distinguished from failure of the corresponding reaction.

Table 1. List of primers used for the amplification of molecular markers of *Plasmodium vivax* and *P. falciparum*.

Target Gene	Reaction	Primer Name	Primer Sequence (5′–3′)	References
18Sr RNA gene	PET-PCR for genus *Plasmodium*	Genus forward	GGC CTA ACA TGG CTA TGA CG	[15,16]
		Genus reverse	6FAM-agg cgc ata gcg cct gg CTG CCT TCC TTA GAT GTG GTA GCT	
18Sr RNA gene	PET-PCR for *P. falciparum*	Falciparum forward	ACC CCT CGC CTG GTG TTT TT	[15]
		Falciparum reverse	HEX-agg cgc ata gcg cct gg TCG GGC CCC AAA AAT AGG AA	
18Sr RNA gene	PET-PCR for *P. vivax*	Vivax forward	ACT GAC ACT GAT GAT TTA GAA CCC ATT T	[20]
		Vivax reverse	HEX- agg cgc ata gcg cct ggT GGA GAG ATC TTT CCA TCC TAA ACC T	
		AL5632	AGG AAT AAA CAA TAA AGA ACA TAA TCA TAC	
pfmsp1 (K1)	1st round	MI-OF	CTA GAA GCT TTA GAA GAT GCA GTA TTG	[5,17]
		MI-OR	CTT AAA TAG ATT CTA ATT CAA GTG GAT CA	
	2nd round	K1F	AAA TGA AGA AGA AAT TAC TAC AAA AGG TGC	
		K1R	GCT TGC ATC AGC TGG AGG GCT TGC ACC AGA	
pfmdr1	SNPs 86, 184	MDR1-1F	TTA AAT GTT TAC CTG CAC AAC ATA GAA AAT T	[11]
		MDR1-1R	CTC CAC AAT AAC TTG CAA CAG TTC TTA	
		MDR1-2F	TGT ATG TGC TGT ATT ATC AGGA	
		MDR1-2R	CTC TTC TAT AAT GGA CAT GGTA	
pfmdr1	SNPs 1034, 1042	1042-A	GTC GAA AAG ACT ATG AAA CGT AGA	[11]
		1042-C	CTC AAA TGA TAA TTT TGC AT	
		1042-B	GAT CCA AGT TTT TTA ATA CA	
		1042-C	CTC AAA TGA TAA TTT TGC AT	

Table 1. *Cont.*

Target Gene	Reaction	Primer Name	Primer Sequence (5′–3′)	References
pvcsp	1st round	VCS-OF	ATG TAG ATC TGT CCA AGG CCA TAA A	[5]
		VCS-OR	TAA TTG AAT AAT GCT AGG ACT AAC AAT ATG	
	2nd round	VCS-NF	GCA GAA CCA AAA AAT CCA CGT GAA AAT AAG	
		VCS-NR	CCA ACG GTA GCT CTA ACT TTA TCT AGG TAT	
pvmsp3α	1st round	Pvmsp3α P1	CAG CAG ACA CCA TTT AAG G	[7,18]
		Pvmsp3α P2	CCG TTT GTT GAT TAG TTG C	
	2nd round	Pvmsp3α N1	GAC CAG TGT GAT ACC ATT AAC C	
		Pvmsp3α N2	ATA CTG GTT CTT CGT CTT CAG G	

PCR products were visualized by agarose gel electrophoresis, purified, and subjected to Sanger sequencing. Raw chromatograms were inspected, edited, and assembled into consensus sequences using Geneious® software v. 2024.0.5. Multiple sequence alignments were generated using ClustalW to identify single nucleotide polymorphisms (SNPs), haplotypes, and sequence variation across samples. For *pfmsp1*, *pvcsp*, and *pfmdr1*, sequences were generated in both forward and reverse directions, and diagnostic polymorphic positions used for haplotype assignment were inspected in the resulting consensus sequences. For *pvmsp3α*, only the sequence generated with the forward primer was available; therefore, haplotype assignment for this marker was based on high-quality, unambiguous forward chromatograms across the trimmed alignment. The resulting sequences were deposited in GenBank, and accession numbers were obtained.

For the *pvcsp* marker, nucleotide sequences were translated in silico to amino acid sequences using the correct open reading frame (ORF) corresponding to the circumsporozoite protein coding region. Translation was performed to confirm sequence integrity and to characterize the composition and order of the nine–amino acid repeat motifs within the central repeat region. The resulting polypeptide sequences were examined to identify non-americ repeat patterns typical of VK210-type alleles and to detect amino acid substitutions among haplotypes. Repeat motif organization was compared across isolates to support haplotype classification at the protein level.

2.4. Genetic Diversity and Structure Analysis

Multiple sequence alignments were first generated for each molecular marker using ClustalW implemented in Geneious® v. 2024.0.5. Genetic diversity indices were then estimated from the aligned nucleotide sequences using DnaSP v5, including the number of haplotypes (h), haplotype diversity (Hd), number of segregating sites (S), average number of nucleotide differences (k), nucleotide diversity (π per site), and Watterson's estimator (θ per site). Alignment positions containing gaps or missing data were excluded from all diversity and neutrality estimates, so the number of sites effectively analysed is smaller than the total alignment length and is reported separately for each marker. Diversity and neutrality analyses were restricted to sequences generated from the 2025 Bay Islands

outbreak samples. Neutrality statistics (Tajima's D and Fu and Li's D* and F*) were computed in DnaSP for both *P. vivax* markers but, because each marker resolved into only two haplotypes and contained no singleton sites, they are reported in Supplementary Table S3 without significance levels and are not interpreted. Previously published Honduran sequences were not pooled with the outbreak dataset because they originated from different periods, locations, and, in some cases, partially overlapping fragments, which could bias diversity estimates.

Clonal expansion was operationally defined as the detection of identical haplotypes, with 100% sequence identity across the analysed fragment, in two or more epidemiologically independent malaria cases at markers used for diversity assessment. For *P. falciparum*, this interpretation was based on *pfmsp1* allelic-family and sequence data; *pfmdr1* was reported separately as a drug-resistance marker and was not used as evidence of restricted diversity. For *P. vivax*, multilocus profiles were based on concordant *pvcsp* and *pvmsp3α* haplotypes. Because only two haplotypes were resolved at each *P. vivax* locus, this operational definition has limited discriminatory power: any two infections carrying the predominant haplotype satisfy it by chance alone. It is therefore applied as a descriptive criterion rather than as a test of common ancestry, and "epidemiologically independent" denotes cases recorded as separate index events by routine surveillance.

Samples showing evidence of mixed infections, defined as the presence of multiple alleles or ambiguous positions in the Sanger sequencing chromatograms, would have been excluded from haplotype-based clustering analyses for the affected marker. Chromatograms were inspected manually in Geneious® software v.2024.0.5 across the trimmed alignments and at all polymorphic positions. A position was considered ambiguous or compatible with a double peak when a secondary peak corresponding to an alternative nucleotide was clearly visible above the local background, occurred at the same nucleotide position as the dominant peak, represented approximately 20–25% or more of the primary peak height, and was not located in a low-quality region or near the read ends. For *pfmsp1*, *pvcsp*, and *pfmdr1*, diagnostic polymorphic positions were inspected in forward and reverse reads; for *pvmsp3α*, only the sequence generated with the forward primer was available, so haplotype assignment was based on high-quality, unambiguous forward chromatograms across the trimmed alignment. No sample met these criteria: no additional alleles and no ambiguous chromatogram positions were detected at any locus, and the proportion of detectable polyclonal infections was therefore zero across the 49 samples analysed. This proportion is reported as a proxy for multiplicity of infection (MOI), the formal assessment of which was not a primary objective of this study.

2.5. Ethical Considerations

This study used anonymized samples collected as part of routine malaria surveillance activities conducted by the Honduran Ministry of Health. No personal identifiers were included in the molecular analyses. In accordance with national regulations governing public health surveillance activities, individual informed consent was not required for the use of these anonymized samples. The study protocol was reviewed and approved by the appropriate institutional and national ethical review committees, in accordance with national regulations and international ethical guidelines (approval PI-10-2025). Ethical approval was obtained after the samples had been collected and is therefore retrospective, as is customary for secondary analyses of anonymized routine surveillance material.

3. Results

3.1. Demographic and Epidemiological Characteristics of Malaria Cases in the Bay Islands

During 2025, a total of 239 confirmed malaria cases were reported in the Bay Islands Department, including 156 cases from JSG, 61 from Roatán, and 22 from Guanaja. Overall, 209 cases (87.4%) were caused by *Plasmodium vivax* and 30 (12.6%) by *P. falciparum*. Of these reported cases, 49 malaria-positive dried blood spot samples (20.5%) were available through routine surveillance and were included in the molecular analysis. The analysed subset comprised 20 samples from Roatán, 15 from JSG, and 14 from Guanaja (Table 2), representing the subset used for all downstream genotyping and haplotype analyses.

Table 2. Demographic and epidemiological characteristics of analysed malaria cases.

Variable	Roatán	JSG	Guanaja	Total
Total confirmed cases reported in 2025	61	156	22	239
Molecularly analysed samples, *n* (%)	20 (32.8%)	15 (9.6%)	14 (63.6%)	49 (20.5%)
Sex, *n* (%)				
• Male	13 (65%)	10 (66.7%)	11 (78.6%)	34 (69.4%)
• Female	7 (35%)	5 (33.3%)	3 (21.4%)	15 (30.6%)
Mean age ± SD	34.6 ± 16.32	33.1 ± 24.01	30.1 ± 15.5	32.8 ± 18.4
Age range (years)	4 to 66	8 to 80	2 to 52	2 to 80
Plasmodium species, *n* (%)				
• *P. vivax*	16 (80%)	15 (100%)	0 (0%)	31 (63.3%)
• *P. falciparum*	4 (20%)	0 (0%)	14 (100%)	18 (36.7%)

Note: The outbreak comprised 239 confirmed malaria cases reported in the Bay Islands Department, Honduras, during 2025, including 156 from José Santos Guardiola (JSG), 61 from Roatán, and 22 from Guanaja. Of these, 49 dried blood spot samples (20.5%) were available and analysed molecularly. The table summarizes the analysed subset by municipality, sex distribution, age, and *Plasmodium* species identified by molecular diagnosis. Percentages are calculated within each municipality.

Within the analysed subset, cases were more frequent among males (34/49; 69.4%), with a comparable sex distribution across municipalities. The mean age was 32.8 years (SD ± 18.4), with a wide age range spanning from 2 to 80 years, indicating involvement of both paediatric and adult populations. Marked differences in *Plasmodium* species distribution were observed by municipality. *P. vivax* infections predominated among samples from Roatán (16/20; 80%) and JSG (15/15; 100%), accounting for 31 analysed samples overall (63.3%). In contrast, *P. falciparum* infections were concentrated in Guanaja (14/14; 100%), with four additional *P. falciparum* samples from Roatán and none from JSG. Thus, Table 2 distinguishes the total outbreak context from the molecularly analysed subset, while Table 3 provides the sample-level temporal distribution and *P. vivax* multilocus haplotype assignment by epidemiological week.

Microscopy-based parasite counts were available for the 49 samples included in the molecular analysis and are provided in Supplementary Table S1. Based on estimated asexual parasite densities, most *P. falciparum* infections showed low parasitaemia, whereas most *P. vivax* infections showed low to moderate parasitaemia, with a small number of high-density infections. Among *P. falciparum* samples, 15/18 were classified as low-density and 3/18 as moderate-density infections. Among *P. vivax* samples, 8/31 were classified as low-density, 17/31 as moderate-density, and 6/31 as high-density infections.

Table 3. Temporal distribution of analysed *Plasmodium vivax* haplotypes.

n	Sample Code	Municipality	Date	Epidemiological Week	*pvcsp* Haplotype	*pvmsp3α* Haplotype	Multilocus Haplotype
1	42	Roatán	4 January	1	B	B	B/B
2	37	Roatán	20 January	4	B	B	B/B
3	38	Roatán	20 January	4	B	B	B/B
4	39	JSG	24 January	4	A	A	A/A
5	43	Roatán	27 January	5	B	B	B/B
6	45	JSG	28 January	5	A	A	A/A
7	44	Roatán	29 January	5	A	A	A/A
8	46	JSG	3 February	6	A	A	A/A
9	47	JSG	7 February	6	A	A	A/A
10	49	JSG	9 February	7	A	A	A/A
11	55	JSG	13 March	11	A	A	A/A
12	57	Roatán	20 March	12	B	B	B/B
13	56	JSG	20 March	12	A	A	A/A
14	59	JSG	27 March	13	A	A	A/A
15	60	JSG	31 March	14	A	A	A/A
16	72	JSG	8 April	15	A	A	A/A
17	78	Roatán	9 April	15	A	A	A/A
18	73	JSG	10 April	15	A	A	A/A
19	74	JSG	11 April	15	A	A	A/A
20	75	JSG	14 April	16	A	A	A/A
21	76	JSG	14 April	16	A	A	A/A
22	79	Roatán	15 April	16	A	A	A/A
23	80	Roatán	15 April	16	A	A	A/A
24	81	Roatán	28 April	18	A	A	A/A
25	82	Roatán	29 April	18	A	A	A/A
26	93	Roatán	14 May	20	A	A	A/A
27	94	Roatán	14 May	20	A	A	A/A
28	95	Roatán	14 May	20	A	A	A/A
29	107	Roatán	9 June	24	A	A	A/A
30	109	Roatán	7 July	28	A	A	A/A
31	110	JSG	11 July	28	A	A	A/A

Note: The table shows the 31 *Plasmodium vivax* samples analysed from the Bay Islands Department, Honduras, during 2025. For each sample, the municipality of detection, date of collection, epidemiological week, *pvcsp* haplotype, *pvmsp3α* haplotype, and combined multilocus haplotype are reported. Haplotypes A and B were assigned based on sequence identity within each marker. The combined *pvcsp*/*pvmsp3α* profile was used to define multilocus haplotypes A/A and B/B and to describe their temporal distribution among analysed samples.

3.2. Molecular Confirmation

Molecular diagnosis by PET-PCR fully confirmed the results obtained by routine diagnostic methods. All 49 samples were positive by genus-specific PET-PCR, and species identification was concordant in all cases. No mixed-species infections were detected. Cycle threshold values ranged from 21 to 39 (median 30) across the 49 samples, from 27 to 38 (median 36) in *P. falciparum* and from 21 to 39 (median 29) in *P. vivax*, and were inversely correlated with microscopy-based asexual parasite density (Pearson r = −0.83 overall; −0.57 in *P. falciparum* and −0.83 in *P. vivax*, on $\log_{10}$-transformed densities), as expected for a quantitative amplification assay. Twelve of the 18 *P. falciparum* samples and 8 of the 31 *P. vivax* samples had Ct $\geq$ 35, reflecting the low parasite densities characteristic of passive case detection in this setting. This complete concordance provided a robust basis for downstream genetic analyses.

3.3. Genetic Diversity of P. falciparum

3.3.1. *P. falciparum* Merozoite Surface Protein 1 (*pfmsp1*)

All 18 *P. falciparum* isolates yielded amplification exclusively of the K1 allelic family, producing an approximately 200 bp PCR product by agarose gel electrophoresis. No MAD20 or RO33 amplification was obtained. MAD20 and RO33 positive controls amplified as expected in every run, so this result reflects the absence of detectable MAD20 and RO33 template rather than failure of the corresponding reactions; minority clones present below the detection threshold of the assay cannot, however, be excluded. After trimming primer-binding regions and low-quality terminal bases from the K1 amplicon sequences, a 178 bp high-quality alignment was retained for haplotype analysis. This trimmed region was identical across all 18 isolates, and only a single K1 haplotype was identified. One representative sequence was deposited in GenBank (accession PX955271).

3.3.2. *P. falciparum* Multidrug Resistance Gene 1 (*pfmdr1*)

Two segments of the *pfmdr1* gene were analysed as drug-resistance markers. The first segment encompassed codons 86 and 184, while the second segment covered codons 1034 and 1042. For the first segment, a 460 bp alignment was obtained, of which 378 positions were free of gaps and missing data, and it was identical across all 18 *P. falciparum* isolates analysed, with no sequence polymorphisms detected among samples. This sequence corresponded to the N86/Y184F haplotype, that is, the wild-type allele at codon 86 and the mutant allele at codon 184 relative to the 3D7 reference sequence. One representative sequence was deposited in GenBank under accession number PX955272. For the second segment, a 288 bp alignment was obtained, of which 282 positions were free of gaps and missing data, and it was likewise identical across all 18 isolates analysed. This sequence corresponded to the S1034C/N1042D haplotype, that is, the mutant allele at both codons relative to the 3D7 reference sequence, with no sequence polymorphisms detected among samples. One representative sequence was deposited in GenBank under accession number PX955273.

3.4. Genetic Diversity of P. vivax Isolates

A total of 31 *P. vivax* isolates were analysed using the *pvcsp* and *pvmsp3α* markers.

3.4.1. *P. vivax* Circumsporozoite Protein (*pvcsp*)

Thirty-one sequences were successfully obtained for *pvcsp*. Two *pvcsp* haplotypes, designated *pvcsp* haplotype A and *pvcsp* haplotype B, were identified. *pvcsp* haplotype A predominated (26/31; 83.9%), while *pvcsp* haplotype B was detected in 5/31 isolates (16.1%). No mixed *pvcsp* genotypes were detected. *pvcsp* haplotype B was detected predominantly during the early phase of transmission in Roatán, with one additional detection in epidemiological week 12. From epidemiological week 13 onward, only *pvcsp* haplotype A was detected among the analysed samples. *pvcsp* haplotype B was not detected among samples collected after epidemiological week 12.

Sequence analysis of the *pvcsp* alignment, which spanned 657 bp in total and retained 593 sites (alignment positions 33–625) after exclusion of positions containing gaps or missing data, identified four segregating sites (S = 4) and two haplotypes (h = 2). Thus, polymorphism in the analysed *pvcsp* fragment was limited, with only four nucleotide substitutions distinguishing the two haplotypes. All four nucleotide substitutions distinguishing the two *pvcsp* haplotypes are shown in Figure 2.

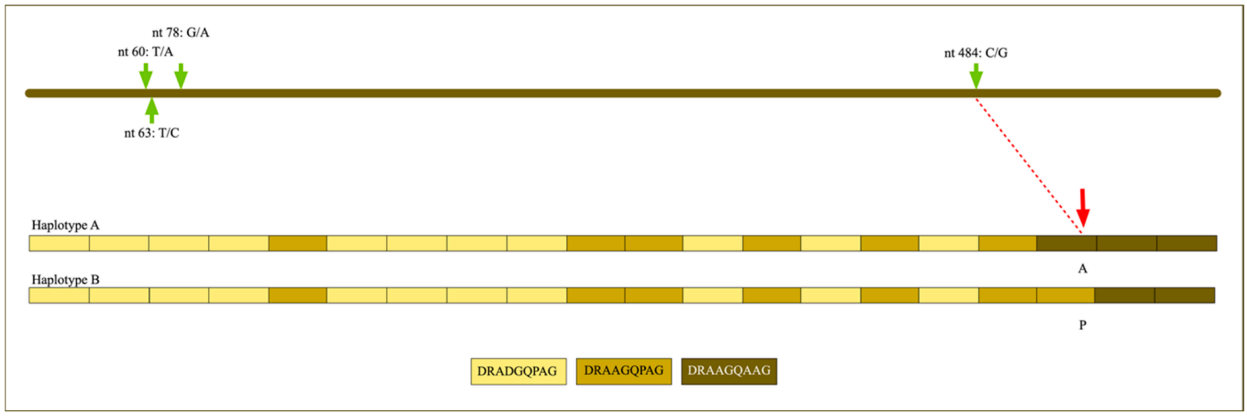


Figure 2. Schematic representation of nucleotide and amino acid polymorphisms in the *pvcsp* gene fragment of the two *P. vivax* haplotypes identified during the outbreak. Note: The upper diagram shows the analysed *pvcsp* nucleotide sequence, with green arrows indicating the single nucleotide polymorphisms detected between haplotypes A and B. The nucleotide changes are indicated above or below each position. The lower diagram shows the organization of the nine–amino acid repeat motifs in the PvCSP central repeat region for haplotypes A and B; each color represents a distinct repeat motif. The red arrow indicates the non-synonymous substitution associated with the amino acid change from alanine (A) in haplotype A to proline (P) in haplotype B. The remaining nucleotide substitutions are shown to document all polymorphic sites observed in the analysed *pvcsp* fragment for molecular surveillance purposes. The red dashed line links the nucleotide substitution at nt 484 to the corresponding amino acid change in the repeat motif.

Haplotype diversity (Hd = 0.2796), and nucleotide diversity were low (π = 0.00189), with an average number of nucleotide differences of k = 1.118. Watterson's estimator per site was θ = 0.00169. Neutrality statistics for this locus are reported in Supplementary Table S3 and are not interpreted, for the reasons given below. These values indicate low haplotype and nucleotide diversity in the analysed *pvcsp* fragment. Representative sequences were deposited in GenBank under accession numbers PZ005775 (haplotype A) and PZ005774 (haplotype B).

The schematic representation of the PvCSP central repeat region (Figure 2) illustrates the organization of the nine–amino acid repeat motifs defining *pvcsp* haplotypes A and B. Both variants shared the canonical repeat structure characteristic of VK210-type sequences, with variation restricted to specific nucleotide and amino acid positions. The principal amino acid difference between haplotypes was localized to the antepenultimate nonapeptide repeat, where a non-synonymous substitution was identified (red arrow). This substitution generated a distinct nine-amino acid repeat motif that served as one of the defining features distinguishing *pvcsp* haplotype B from *pvcsp* haplotype A, while the remaining repeat blocks were conserved between variants.

3.4.2. *P. vivax* Merozoite Protein 3 Alpha (*pvmsp3α*)

Analysis of the *pvmsp3α* alignment, which spanned 723 bp in total and retained 336 sites (46.5% of the alignment; alignment positions 16–371) after exclusion of positions containing gaps or missing data, identified 37 segregating sites (S = 37) and two haplotypes (h = 2), corresponding to the same 26/5 sample split observed at *pvcsp*. Because haplotype diversity depends only on sample size and haplotype frequencies, Hd was numerically identical to that of *pvcsp* (Hd = 0.2796), despite the much larger number of segregating sites distinguishing the two *pvmsp3α* haplotypes. Nucleotide diversity was higher than at *pvcsp* (π = 0.03079), with an average of k = 10.344 nucleotide differences, and Watterson's estimator per site was θ = 0.02756. Neutrality statistics for this locus are likewise reported in Supplementary Table S3 and are not interpreted.

Because each *P. vivax* marker resolved into only two haplotypes, every segregating site partitions the sample in the same way, at 26 and 5 sequences, and no site is a singleton. All of the observed variation therefore maps onto a single internal branch of the genealogy, so Tajima's D and Fu and Li's D* and F* are not estimated from the configuration their null distributions assume, and in the absence of singleton sites Fu and Li's D* and F* are positive by construction irrespective of population history. These statistics are consequently reported in Supplementary Table S3 for completeness, without significance levels, and are not used as evidence of demographic change or of selection anywhere in this study.

Despite the nucleotide-level variation and the presence of multiple segregating sites, most sequences corresponded to a single dominant haplotype. Representative sequences were deposited under accession numbers PX955277 (haplotype A) and PX955276 (haplotype B).

3.5. Multilocus Structure and Clonal Patterns in P. vivax

The combined *pvcsp/pvmsp3α* analysis showed complete concordance between markers, with samples assigned to either multilocus haplotype A/A or B/B (Table 3). The predominant detected multilocus haplotype corresponded to haplotype A at both loci (A/A). From epidemiological week 13 onward, A/A was the only multilocus haplotype detected among successfully genotyped *P. vivax* infections across both Roatán and JSG (Figure 3). However, this temporal pattern should be interpreted cautiously because B/B was detected in only five samples overall, and low sampling density or stochastic sampling could have contributed to its apparent absence later in the sampling period. Therefore, the temporal distribution shown in Figure 3 refers only to the subset of samples included in the molecular analysis and should be interpreted as the temporal distribution of detected genotyped infections rather than as a complete epidemic curve of all reported malaria cases in the department.

By the operational descriptive definition applied in this study, the repeated detection of a single *pfmsp1* K1 haplotype among analysed *P. falciparum* isolates, together with the predominance of the A/A multilocus haplotype among analysed *P. vivax* infections, was compatible with marker-level focal amplification. This marker-based pattern should not be interpreted as genomic-level clonality, which was not assessed in this study.

Multilocus haplotype B/B was detected in five analysed samples, all from Roatán, mainly during the early phase of transmission, with one additional detection in epidemiological week 12. This haplotype was not detected among the analysed samples collected after epidemiological week 12. However, given the limited number of B/B detections and the subset of cases available for molecular analysis, this apparent temporal pattern should not be interpreted as definitive evidence of lineage replacement. No additional multilocus haplotypes were identified among the analysed samples during the later sampling period. Restricting the comparison to Roatán, the only municipality in which B/B was detected and therefore the stratum in which the temporal contrast is not confounded by municipality, B/B accounted for five of six genotyped *P. vivax* infections during epidemiological weeks 1–12 and for none of the ten infections genotyped from week 13 onward (Fisher's exact test, $p = 0.0014$). Because the cut-point was chosen after inspection of the data and the comparison rests on five events, this value describes the observed distribution and is not presented as a formal test of lineage turnover. Within the analysed subset, A/A accounted for 11 of 16 genotyped *P. vivax* infections in Roatán and for all 15 in JSG, although JSG contributed 156 of the 239 reported cases and only 9.6% of them were genotyped.

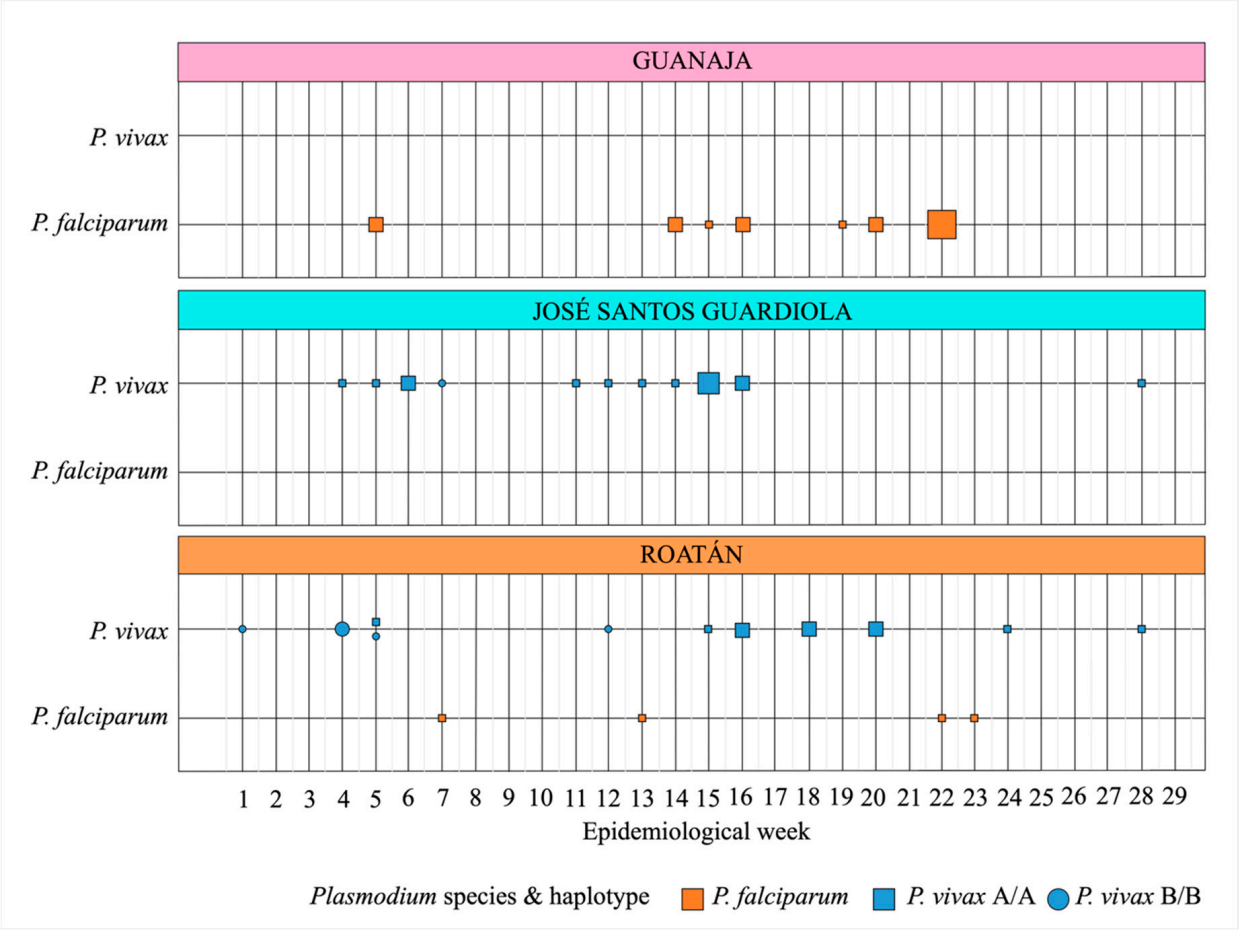


Figure 3. Temporal distribution of molecularly analysed malaria samples by epidemiological week in the Bay Islands Department, Honduras, 2025. Symbols depict *Plasmodium vivax* and *P. falciparum* samples included in the molecular analysis by epidemiological week, municipality, parasite species, and multilocus haplotype. For *P. vivax*, symbol shape indicates the multilocus haplotype based on concordant *pvcsp* and *pvmsp3α* genotyping: squares represent A/A and circles represent B/B. Orange squares represent *P. falciparum* samples, all of which carried the same *pfmsp1* K1 haplotype. Symbol size is proportional to the number of molecularly analysed samples for each epidemiological week, municipality, species, and haplotype category.

Overall, all *P. falciparum* isolates carried a single *pfmsp1* K1 haplotype, whereas *P. vivax* samples showed two concordant multilocus haplotypes, with A/A becoming the predominant detected multilocus haplotype among the analysed samples.

4. Discussion

The molecular analyses conducted during the 2025 phase of the malaria outbreak in the Bay Islands, Honduras, revealed a markedly restricted genetic profile among the analysed parasites. *Plasmodium falciparum* isolates carried a single *pfmsp1* K1 haplotype, whereas *P. vivax* was characterized by two detected multilocus haplotypes with complete concordance between *pvcsp* and *pvmsp3α*. The A/A multilocus haplotype became the predominant detected profile among analysed *P. vivax* samples later in the sampling period. Together, these findings indicate reduced allelic diversity and a constrained parasite genetic profile within a geographically confined setting. In a region committed to malaria elimination by 2030 [2], such patterns should be interpreted within the broader context of declining transmission, focal persistence, and the limited resolution of targeted molecular markers.

In this study, "local expansion" refers to focal amplification within the Bay Islands outbreak setting, rather than to independent clonal expansion within each municipality. This distinction is important because multilocus haplotypes, particularly the predominant *P. vivax* A/A profile, were shared between Roatán and JSG. Therefore, the observed pattern supports restricted diversity at the departmental outbreak scale but should not be interpreted as evidence of genetically differentiated municipal transmission units. Shared haplotypes may reflect epidemiological connectivity, human movement, common source populations, or limited marker resolution. Accordingly, the results are best interpreted as being consistent with focal amplification of genetically constrained parasite lineages within the Bay Islands, without excluding repeated introductions of closely related parasites.

Across Mesoamerica and Hispaniola, sustained reductions in malaria incidence over the past two decades [21] have led to increasingly focal transmission, with cases concentrated in residual hotspots. As transmission declines, parasite populations may contract, recombination opportunities decrease, and infections can become more spatially structured [3,22–25]. Under such conditions, small transmission foci may amplify from a limited ancestral pool, particularly in ecologically receptive areas [24,26,27]. Insular transmission systems such as the Bay Islands may be especially vulnerable to these dynamics: restricted gene flow and geographic isolation can magnify founder effects once transmission is re-established, while high ecological receptivity favors rapid amplification of the founding lineage thereafter [28]. Thus, the genetic homogeneity observed here is compatible with expectations for malaria resurgence in low-transmission, geographically constrained environments.

The 2025 outbreak also occurred in a national context of reduced parasite diversity. Previous studies in Honduras have documented progressive contraction of parasite genetic diversity during the elimination phase, including reduced multiplicity of infection, dominance of specific haplotypes, and evidence of demographic bottlenecks in *P. falciparum* populations along the Honduran–Nicaraguan border [3–7,12,13]. Earlier molecular studies have also shown limited but persistent diversity in both *P. falciparum* and *P. vivax* populations [7,12,13]. In the present study, the *pvcsp* allelic profiles detected in the Bay Islands were compatible with VK210-type variants previously reported in Honduras [5], and the restricted *pvmsp3α* diversity was consistent with the reduced haplotypic richness previously reported in Honduran field isolates [7]. Neutrality statistics were not used to support any demographic interpretation. With only two haplotypes and no singleton sites at either *P. vivax* locus, these tests have no interpretable null distribution in this dataset, and the positive values of Fu and Li's D* and F* follow algebraically from the absence of singletons rather than from population history. The demographic contraction invoked here therefore rests on the published Honduran evidence cited above, not on the neutrality statistics of the present dataset.

Similarly, the uniform *pfmdr1* profile detected among outbreak isolates was consistent with the limited *pfmdr1* variation previously documented in Honduras and Nicaragua [11]. These comparisons suggest that the outbreak-associated haplotypes may belong to parasite lineages already circulating in Honduras; however, without formal phylogenetic, microsatellite, or genome-wide analyses, this remains an inference rather than a demonstrated conclusion. Because that haplotype was fixed in every Honduran and Nicaraguan isolate previously sequenced, its uniformity in the present series is the expected outcome under any transmission scenario, including repeated importation, and it is accordingly reported as a drug-resistance result rather than as evidence of focal amplification.

The different levels of polymorphism observed between *pvcsp* and *pvmsp3α* should be interpreted in light of their distinct evolutionary characteristics. In this study, *pvcsp* showed limited nucleotide variation, whereas *pvmsp3α* displayed a higher number of segregating sites despite resolving into the same two haplotypes at identical frequencies. This pattern is compatible with the higher polymorphism expected for *pvmsp3α*. Therefore, the concordant A/A and B/B profiles support restricted multilocus diversity among the analysed samples but do not prove that all infections derived from a single recent lineage. Higher-resolution comparative analyses would be required to determine the precise evolutionary relationships among these haplotypes.

The relapsing biology of *P. vivax* offers a further explanation that the present data cannot exclude. Because hypnozoites may reactivate weeks to months after the primary infection, the later predominance of the A/A multilocus haplotype could reflect recurrent parasitaemia in a limited group of patients infected early in the outbreak rather than sustained vector-borne transmission of that lineage. Individual-level data on treatment adherence and on completion of radical cure with primaquine were not systematically available, and no genotyping of paired recurrent samples was performed, so relapse could not be distinguished from reinfection or from new transmission. Unmonitored relapses would inflate the apparent frequency of the predominant haplotype over time and would therefore reinforce, artefactually, the temporal pattern described here.

The Bay Islands pattern contrasts with moderate- to high-transmission settings, where polyclonal infections, high multiplicity of infection, and greater allelic richness are commonly reported [29,30]. Similarly, in parts of Southeast Asia with ongoing but unstable transmission, *pvcsp* and *pvmsp3α* loci often display substantial haplotypic diversity and multiple co-circulating genotypes [31,32]. In contrast, the restricted diversity observed in the Bay Islands resembles patterns reported from pre-elimination or post-interruption settings. Examples include *P. vivax* outbreaks in Suriname associated with persistence and expansion of a single lineage [26]; *P. falciparum* resurgence in eastern Panama involving highly related parasite subpopulations [24]; clonal signatures in Cape Verde based on genome-wide similarity [27]; and limited *pvcsp* diversity in southern Thailand [33]. These comparisons support the interpretation that low-transmission settings may favor amplification of a limited number of parasite lineages, although the targeted markers used here do not allow definitive demonstration of genomic clonality.

The more informative comparison, however, is with the Honduran mainland, where the same markers have been applied during the same elimination period (Table S2). All three *pfmsp1* allelic families circulate on the mainland, 23 size-based alleles were resolved among 30 isolates in 2010–2011 [5], and polyclonal infection is common, reaching 65.3% of isolates along the Honduran–Nicaraguan border in 2018–2021 [3]. The outbreak isolates, by contrast, yielded a single *pfmsp1* sequence haplotype restricted to the K1 family, with no polyclonal infection detected. The same direction is seen in *P. vivax*, where 23 *pvcsp* allelic types have been reported nationally [5] against the two haplotypes detected here, and seven *pvmsp3α* nucleotide haplotypes were resolved in the national series typed with that marker [7] against the two detected in this outbreak. Because fragment boundaries and typing approaches differ between studies, these contrasts are descriptive rather than formally comparable diversity estimates; nonetheless, they indicate that the restriction observed in the Bay Islands is not simply the national baseline. It should also be noted that ref. [3] found no sequence polymorphism within *pfmsp1* allelic subfamilies, so the sequence-level uniformity observed here adds little information beyond the loss of allelic-family diversity, and that ref. [7] reported no geographical clustering of *P. vivax* haplotypes within Honduras, which is a further reason why shared haplotypes between municipalities cannot by themselves establish a single local source.

The epidemiological interpretation of the Bay Islands outbreak should therefore remain cautious. For *P. falciparum*, the detection of a single *pfmsp1* sequence haplotype, restricted to the K1 allelic family, is compatible with focal amplification of a limited number of lineages; the uniform *pfmdr1* profile is not informative in this respect, since the same haplotype has been reported in every Honduran and Nicaraguan isolate previously sequenced.

For *P. vivax*, the presence of two concordant multilocus haplotypes and the predominance of A/A among detected infections later in the sampling period indicate restricted multilocus diversity among analysed samples. However, these findings do not prove a single source, strict spatial confinement, or definitive lineage replacement. Because systematic travel-history data, individual-level mobility information, population-structure analyses, and genome-wide comparisons with contemporaneous parasites from mainland Honduras or neighboring regions were not available, multiple introductions of genetically similar parasites cannot be excluded. Studies from Mexico and Panama have shown that residual malaria foci may exhibit genetic differentiation even across geographically proximate areas [34,35] but the present study did not include comparable population differentiation analyses. The spatial patterns observed here should therefore be considered descriptive evidence of restricted detected diversity rather than proof of genetically differentiated transmission compartments.

The programmatic implications remain relevant. In elimination settings, routine surveillance indicators cannot reliably distinguish importation-driven outbreaks from local amplification of genetically similar parasites. Molecular genotyping can add useful resolution to outbreak investigations, as emphasized in regional experiences from Costa Rica and other low-endemic settings [36,37]. In insular contexts such as the Bay Islands, where ecological receptivity remains high and *Anopheles albimanus* persists [38], early detection of restricted parasite diversity may help guide targeted response activities. Future studies incorporating broader temporal sampling, whole-genome or microsatellite data, travel histories, and comparison with mainland parasite populations will be necessary to distinguish focal amplification from repeated introductions and to refine molecular surveillance strategies for malaria elimination in Honduras and the wider Mesoamerican region.

Limitations

This study has limitations. Genotyping was based on targeted Sanger sequencing of selected markers rather than whole-genome sequencing; therefore, the observed homogeneity should be interpreted as restricted diversity at the analysed loci, not as definitive evidence of genomic clonality, and low-frequency subclonal variants may have been missed. The molecular dataset also represented only a subset of reported cases: 49 of 239 cases overall, including 18 of 30 *P. falciparum* cases and 31 of 209 *P. vivax* cases. Thus, minority lineages or less frequent haplotypes, particularly in *P. vivax*, may have been missed. Molecular data were unavailable from the initial 2024 outbreak phase, and previous Honduran haplotypes could not determine whether the 2025 haplotypes had circulated previously at high or low frequency. The *pvmsp3α* window analysed here is also narrower than the amplicon length implies. Of the 723 alignment positions, 336 (46.5%) were retained after exclusion of gaps and missing data; the retained window lies in the 5′ half of the amplicon, spanning alignment positions 16 to 371, and its 3′ boundary is set by the two shortest reads in the set, samples 73 and 93, whose sequences end at alignment positions 371 and 374. Excluding those two sequences would extend the window to 370 sites and increase the number of segregating sites from 37 to 45, so the diversity estimate at this locus is governed by the two shortest reads. Because only the forward read was available at *pvmsp3α*, the double-peak criterion used to screen for mixed infections operated on a single direction at this locus,

whereas at *pfmsp1*, *pvcsp* and *pfmdr1* the secondary signal had to be visible in both directions; the screen is therefore weaker at the one marker that carries 37 of the 41 segregating sites detected in this study. Comparisons with published *pvmsp3α* diversity should accordingly be read against this single-direction 336-site window rather than against the full 723 bp alignment. Neutrality statistics were not interpreted at either *P. vivax* locus, for the reasons given in the Results and in Supplementary Table S3. Finally, individual-level treatment adherence, longitudinal follow-up, travel history, and mobility data were unavailable; therefore, *P. vivax* relapse or recurrent parasitaemia could not be formally assessed, and multiple introductions of genetically similar parasite lineages cannot be excluded. Future studies using broader sampling, genomic approaches, treatment follow-up, relapse assessment, and mobility data would refine understanding of parasite dynamics in insular elimination settings. The size of the analysed subset also sets a floor on what could have been detected: with 31 *P. vivax* and 18 *P. falciparum* samples, a haplotype circulating at a frequency of 9.2% or less in *P. vivax*, or of 15.3% or less in *P. falciparum*, could have escaped detection with 95% confidence. Coverage was moreover uneven across foci, reaching 63.6% of reported cases in Guanaja and 32.8% in Roatán but only 9.6% in JSG, the municipality that contributed 65% of all reported cases, so the dominant A/A signal rests on the least intensively sampled focus. Finally, all four loci encode surface antigens or drug-resistance targets and are therefore subject to selection, which further limits their use for demographic inference. A related constraint concerns template abundance: 12 of the 18 *P. falciparum* samples were amplified from material with a PET-PCR Ct of 35 or higher, and at such low template input a minority clone present at a small fraction of the total parasite population could fail to amplify or fall below the threshold for detection as a double peak in the sequencing chromatogram. The absence of polyclonal infection reported here should therefore be read as absence of detectable polyclonality with the methods used, and not as proof that every infection was monoclonal.

5. Conclusions

The 2025 phase of the malaria outbreak in the Bay Islands of Honduras was characterized by marked genetic homogeneity in *P. falciparum* and restricted multilocus diversity in *P. vivax*, including temporal predominance of a single *P. vivax* multilocus haplotype among the analysed samples. Although the targeted markers used in this study do not allow definitive demonstration of clonal expansion in the genomic sense, the observed patterns are consistent with focal amplification of a limited number of parasite lineages within a geographically confined, low-transmission setting. In the context of sustained malaria reduction and prior evidence of demographic contraction of parasite populations in Honduras, these findings suggest that the outbreak involved circulation and expansion of genetically constrained parasite lineages, although repeated introductions of genetically similar parasites cannot be excluded with the markers used here. Our results highlight the value of multilocus molecular surveillance for characterizing outbreak-associated parasite diversity, supporting interpretation of local transmission dynamics, and informing evidence-based malaria elimination strategies in Honduras and the wider Mesoamerican region.

Supplementary Materials: The following supporting information can be downloaded at: https://www.mdpi.com/article/10.3390/parasitologia6050053/s1, Supplementary Table S1. Microscopy-based parasite counts and estimated parasite densities among malaria-positive samples included in the molecular analysis. Supplementary Table S2. Genotypes detected during the 2025 Bay Islands outbreak compared with previously reported Honduran datasets using the same molecular markers. Supplementary Table S3. Neutrality statistics for the *P. vivax* markers, reported without significance levels. Supplementary Data S1. *pfmsp1* nucleotide alignment. Supplementary Data S2. *pfmdr1* codons

86 and 184 nucleotide alignment. Supplementary Data S3. *pfmdr1* codons 1034 and 1042 nucleotide alignment. Supplementary Data S4. *pvcsp* nucleotide alignment. Supplementary Data S5. *pvmsp3α* nucleotide alignment.

Author Contributions: G.F.: Conceptualization, methodology validation, formal analysis, data curation, visualization, writing—original draft, supervision, project administration. F.P., D.E., G.A., L.C.: Methodology, investigation, writing—review and editing. H.O.V., G.F.: Resources, funding acquisition. L.C., G.A., A.M., D.O., M.C.: Epidemiological surveillance and field follow-up of the malaria outbreak in the Bay Islands. D.E., G.F.: Project administration. All authors have read and agreed to the published version of the manuscript.

Funding: Funding for this study was provided by the Genetic Research Center, CIG-UNAH, and by the Armed Forces Health Surveillance Division (AFHSD), Global Emerging Infections Surveillance (GEIS) Branch (PROMIS ID P0146_25_N6). The funders had no role in study design, data collection, analysis, decision to publish, or preparation of the manuscript. The APC was funded by DICIHT-UNAH.

Institutional Review Board Statement: The study protocol was reviewed and approved by the appropriate institutional and national ethical review committees, in accordance with national regulations and international ethical guidelines (approval PI-10-2025).

Informed Consent Statement: This study used anonymized samples collected as part of routine malaria surveillance activities conducted by the Honduran Ministry of Health. No personal identifiers were included in the molecular analyses. In accordance with national regulations governing public health surveillance activities, individual informed consent was not required for the use of these anonymized samples.

Data Availability Statement: All representative nucleotide haplotypes generated in this study have been deposited in GenBank under the accession numbers reported in the Section 3. Complete multiple sequence alignments for all analysed markers are provided as Supplementary Data, including sample-level sequences used for haplotype assignment, identification of polymorphic sites, and estimation of diversity indices. Additional data supporting the findings of this study are available from the corresponding author upon reasonable request.

Conflicts of Interest: One of the authors of this manuscript (H.O.V.) is an employee of the U.S. Government. This work was prepared as part of his official duties. Title 17 U.S.C. §105 provides that "Copyright protection under this Title is not available for any work of the United States Government". Title 17 U.S.C. §101 defines a U.S. Government work as a work prepared by a military service member or employee of the U.S. Government as part of that person's official duties. The views expressed in this article are those of the authors and do not necessarily reflect the official policy or position of the Department of the Navy, Department of Defense, nor the U.S. Government.

Abbreviations

The following abbreviations are used in this manuscript:

ACT	Artemisinin-based combination therapy
CIG-UNAH	Centro de Investigaciones Genéticas—Universidad Nacional Autónoma de Honduras
Hd	Haplotype diversity
JSG	José Santos Guardiola
k	Average number of nucleotide differences
MAD20	Merozoite surface protein 1 allelic family MAD20
MOI	Multiplicity of infection
ORF	Open reading frame
PET-PCR	Photo-induced electron transfer polymerase chain reaction
Pf	*Plasmodium falciparum*
pfmdr1	*Plasmodium falciparum* multidrug resistance gene 1

pfmsp1	*Plasmodium falciparum* merozoite surface protein 1
Pv	*Plasmodium vivax*
pvcsp	*Plasmodium vivax* circumsporozoite protein gene
pvmsp3α	*Plasmodium vivax* merozoite surface protein 3 alpha gene
SNP	Single nucleotide polymorphism
RDT	Rapid diagnostic test
VK210	*Plasmodium vivax* circumsporozoite protein VK210 variant
VK247	*Plasmodium vivax* circumsporozoite protein VK247 variant

References

1. Mecanismo Coordinador de País. Honduras (MCP-H). Subvención Malaria del 1 de Enero del 2024 al 31 de Diciembre de 2025. Available online: https://mcp-honduras.hn/malaria/ (accessed on 13 February 2026).
2. World Health Organization. *Global Technical Strategy and Targets for Malaria 2016–2030*; WHO: Geneva, Switzerland, 2015.
3. Pinto, A.; Archaga, O.; Mejia, A.; Escober, L.; Henriquez, J.; Montoya, A.; Valdivia, H.O.; Fontecha, G. Evidence of a Recent Bottleneck in *Plasmodium falciparum* Populations on the Honduran-Nicaraguan Border. *Pathogens* **2021**, *10*, 1432. [CrossRef] [PubMed]
4. Haddad, D.; Snounou, G.; Mattei, D.; Enamorado, I.G.; Figueroa, J.; Stahl, S.; Berzins, K. Limited genetic diversity of *Plasmodium falciparum* in field isolates from Honduras. *Am. J. Trop. Med. Hyg.* **1999**, *60*, 30–34. [CrossRef] [PubMed]
5. Lopez, A.C.; Ortiz, A.; Coello, J.; Sosa-Ochoa, W.; Torres, R.E.; Banegas, E.I.; Jovel, I.; Fontecha, G.A. Genetic diversity of *Plasmodium vivax* and *Plasmodium falciparum* in Honduras. *Malar. J.* **2012**, *11*, 391. [CrossRef] [PubMed]
6. Larranaga, N.; Mejia, R.E.; Hormaza, J.I.; Montoya, A.; Soto, A.; Fontecha, G.A. Genetic structure of *Plasmodium falciparum* populations across the Honduras-Nicaragua border. *Malar. J.* **2013**, *12*, 354. [CrossRef] [PubMed]
7. Zamora, A.; Pinto, A.; Escobar, D.; Valdivia, H.O.; Chaver, L.; Ardon, G.; Carranza, E.; Fontecha, G. Genetic diversity of *Plasmodium vivax* and *Plasmodium falciparum* field isolates from Honduras in the malaria elimination phase. *Curr. Res. Parasitol. Vector Borne Dis.* **2025**, *7*, 100230. [CrossRef] [PubMed]
8. Chen, Y.A.; Ng, P.Y.; Garcia-Ruiz, D.; Elliot, A.; Palmer, B.; Assuncao Carvalho, R.M.C.; Tseng, L.F.; Lee, C.S.; Tsai, K.H.; Greenhouse, B.; et al. Genetic surveillance reveals low but sustained malaria transmission with clonal replacement in Sao Tome and Principe. *Commun. Med.* **2025**, *5*, 199. [CrossRef] [PubMed]
9. Noviyanti, R.; Coutrier, F.; Utami, R.A.; Trimarsanto, H.; Tirta, Y.K.; Trianty, L.; Kusuma, A.; Sutanto, I.; Kosasih, A.; Kusriastuti, R.; et al. Contrasting Transmission Dynamics of Co-endemic *Plasmodium vivax* and *P. falciparum*: Implications for Malaria Control and Elimination. *PLoS Negl. Trop. Dis.* **2015**, *9*, e0003739. [CrossRef] [PubMed]
10. Ruybal-Pesantez, S.; McCann, K.; Vibin, J.; Siegel, S.; Auburn, S.; Barry, A.E. Molecular markers for malaria genetic epidemiology: Progress and pitfalls. *Trends Parasitol.* **2024**, *40*, 147–163. [CrossRef] [PubMed]
11. Fontecha, G.; Pinto, A.; Archaga, O.; Betancourth, S.; Escober, L.; Henriquez, J.; Valdivia, H.O.; Montoya, A.; Mejia, R.E. Assessment of *Plasmodium falciparum* anti-malarial drug resistance markers in pfcrt and *pfmdr1* genes in isolates from Honduras and Nicaragua, 2018–2021. *Malar. J.* **2021**, *20*, 465. [CrossRef] [PubMed]
12. Banegas, S.; Escobar, D.; Pinto, A.; Moncada, M.; Matamoros, G.; Valdivia, H.O.; Reyes, A.; Fontecha, G. Asymptomatic Malaria Reservoirs in Honduras: A Challenge for Elimination. *Pathogens* **2024**, *13*, 541. [CrossRef] [PubMed]
13. Godoy, A.; Euceda, K.; Pinto, A.; Valdivia, H.O.; Chaver, L.; Ardon, G.; Fontecha, G. Molecular Characterization of *Plasmodium* Species to Strengthen Malaria Surveillance in Migrant Populations in Honduras. *Trop. Med. Infect. Dis.* **2025**, *10*, 292. [CrossRef] [PubMed]
14. Lucchi, N.W.; Karell, M.A.; Journel, I.; Rogier, E.; Goldman, I.; Ljolje, D.; Huber, C.; Mace, K.E.; Jean, S.E.; Akom, E.E.; et al. PET-PCR method for the molecular detection of malaria parasites in a national malaria surveillance study in Haiti, 2011. *Malar. J.* **2014**, *13*, 462. [CrossRef] [PubMed]
15. Lucchi, N.W.; Narayanan, J.; Karell, M.A.; Xayavong, M.; Kariuki, S.; DaSilva, A.J.; Hill, V.; Udhayakumar, V. Molecular diagnosis of malaria by photo-induced electron transfer fluorogenic primers: PET-PCR. *PLoS ONE* **2013**, *8*, e56677. [CrossRef] [PubMed]
16. Matamoros, G.; Escobar, D.; Pinto, A.; Serrano, D.; Ksandrova, E.; Grimaldi, N.; Juarez-Fontecha, G.; Moncada, M.; Valdivia, H.O.; Fontecha, G. PET-PCR reveals low parasitaemia and submicroscopic malarial infections in Honduran Moskitia. *Malar. J.* **2023**, *22*, 110. [CrossRef] [PubMed]
17. Snounou, G.; Zhu, X.; Siripoon, N.; Jarra, W.; Thaithong, S.; Brown, K.N.; Viriyakosol, S. Biased distribution of *msp1* and *msp2* allelic variants in *Plasmodium falciparum* populations in Thailand. *Trans. R. Soc. Trop. Med. Hyg.* **1999**, *93*, 369–374. [CrossRef] [PubMed]

18. Thanapongpichat, S.; Khammanee, T.; Sawangjaroen, N.; Buncherd, H.; Tun, A.W. Genetic Diversity of *Plasmodium vivax* in Clinical Isolates from Southern Thailand using PvMSP1, PvMSP3 (PvMSP3alpha, PvMSP3beta) Genes and Eight Microsatellite Markers. *Korean J. Parasitol.* **2019**, *57*, 469–479. [CrossRef] [PubMed]
19. Jovel, I.T.; Mejia, R.E.; Banegas, E.; Piedade, R.; Alger, J.; Fontecha, G.; Ferreira, P.E.; Veiga, M.I.; Enamorado, I.G.; Bjorkman, A.; et al. Drug resistance associated genetic polymorphisms in *Plasmodium falciparum* and *Plasmodium vivax* collected in Honduras, Central America. *Malar. J.* **2011**, *10*, 376. [CrossRef] [PubMed]
20. Kudyba, H.M.; Louzada, J.; Ljolje, D.; Kudyba, K.A.; Muralidharan, V.; Oliveira-Ferreira, J.; Lucchi, N.W. Field evaluation of malaria malachite green loop-mediated isothermal amplification in health posts in Roraima state, Brazil. *Malar. J.* **2019**, *18*, 98. [CrossRef] [PubMed]
21. World Health Organization. *World Malaria Report 2024*; WHO: Geneva, Switzerland, 2024; p. 316.
22. Griffing, S.; Syphard, L.; Sridaran, S.; McCollum, A.M.; Mixson-Hayden, T.; Vinayak, S.; Villegas, L.; Barnwell, J.W.; Escalante, A.A.; Udhayakumar, V. *pfmdr1* amplification and fixation of *pfcrt* chloroquine resistance alleles in *Plasmodium falciparum* in Venezuela. *Antimicrob. Agents Chemother.* **2010**, *54*, 1572–1579. [CrossRef] [PubMed]
23. Vo, T.C.; Le, H.G.; Kang, J.M.; Trinh, N.T.M.; Quang, H.H.; Na, B.K. Genetic polymorphism of merozoite surface protein 1 and merozoite surface protein 2 in the Vietnam *Plasmodium falciparum* population. *BMC Infect. Dis.* **2024**, *24*, 1216. [CrossRef] [PubMed]
24. Obaldia, N., 3rd; Baro, N.K.; Calzada, J.E.; Santamaria, A.M.; Daniels, R.; Wong, W.; Chang, H.H.; Hamilton, E.J.; Arevalo-Herrera, M.; Herrera, S.; et al. Clonal outbreak of *Plasmodium falciparum* infection in eastern Panama. *J. Infect. Dis.* **2015**, *211*, 1087–1096. [CrossRef] [PubMed]
25. Saenz, F.E.; Morton, L.C.; Okoth, S.A.; Valenzuela, G.; Vera-Arias, C.A.; Velez-Alvarez, E.; Lucchi, N.W.; Castro, L.E.; Udhayakumar, V. Clonal population expansion in an outbreak of *Plasmodium falciparum* on the northwest coast of Ecuador. *Malar. J.* **2015**, *14*, 497. [CrossRef] [PubMed]
26. Labadie-Bracho, M.Y.; Adhin, M.R. Reconstruction of *Plasmodium vivax* outbreaks in a low malaria endemic setting utilizing conventional restriction fragment length polymorphism. *Int. J. Mol. Epidemiol. Genet.* **2021**, *12*, 9–15. [PubMed]
27. Da Veiga Leal, S.; Ward, D.; Campino, S.; Benavente, E.D.; Ibrahim, A.; Claret, T.; Isaias, V.; Monteiro, D.; Clark, T.G.; Goncalves, L.; et al. Drug resistance profile and clonality of *Plasmodium falciparum* parasites in Cape Verde: The 2017 malaria outbreak. *Malar. J.* **2021**, *20*, 172. [CrossRef] [PubMed]
28. Huang, B.; Tuo, F.; Liang, Y.; Wu, W.; Wu, G.; Huang, S.; Zhong, Q.; Su, X.Z.; Zhang, H.; Li, M.; et al. Temporal changes in genetic diversity of *msp-1*, *msp-2*, and *msp-3* in *Plasmodium falciparum* isolates from Grande Comore Island after introduction of ACT. *Malar. J.* **2018**, *17*, 83. [CrossRef] [PubMed]
29. Simpson, S.V.; Nundu, S.S.; Arima, H.; Kaneko, O.; Mita, T.; Culleton, R.; Yamamoto, T. The diversity of *Plasmodium falciparum* isolates from asymptomatic and symptomatic school-age children in Kinshasa Province, Democratic Republic of Congo. *Malar. J.* **2023**, *22*, 102. [CrossRef] [PubMed]
30. Andika, B.; Mobegi, V.; Gathii, K.; Nyataya, J.; Maina, N.; Awinda, G.; Mutai, B.; Waitumbi, J. *Plasmodium falciparum* population structure inferred by *msp1* amplicon sequencing of parasites collected from febrile patients in Kenya. *Malar. J.* **2023**, *22*, 263. [CrossRef] [PubMed]
31. Vo, T.C.; Trinh, N.T.M.; Le, H.G.; Kang, J.M.; Yoo, W.G.; Quang, H.H.; Na, B.K. Genetic Diversity of Circumsporozoite Surface Protein of *Plasmodium vivax* from the Central Highlands, Vietnam. *Pathogens* **2022**, *11*, 1158. [CrossRef] [PubMed]
32. Hayat, C.; Kamil, A.; Khan, A.; Sayed, A.; Akbar, K.; Afridi, S.G. Genetic diversity of *Plasmodium falciparum* and *Plasmodium vivax* field isolates from the Nowshera district of Pakistan. *Malar. J.* **2024**, *23*, 358. [CrossRef] [PubMed]
33. Khulmanee, T.; Thita, T.; Kritsiriwutinan, K.; Boonyuen, U.; Saai, A.; Inkabjan, K.; Chakrabarti, R.; Rathod, P.K.; Krudsood, S.; Mungthin, M.; et al. Low Genetic Diversity of *Plasmodium vivax* Circumsporozoite Surface Protein in Clinical Isolates from Southern Thailand. *Trop. Med. Infect. Dis.* **2024**, *9*, 94. [CrossRef] [PubMed]
34. Santamaria, A.M.; Vasquez, V.; Rigg, C.; Samudio, F.; Moreno, D.; Romero, L.; Saldana, A.; Chaves, L.F.; Calzada, J.E. *Plasmodium vivax* Genetic Diversity in Panama: Challenges for Malaria Elimination in Mesoamerica. *Pathogens* **2021**, *10*, 989. [CrossRef] [PubMed]
35. Gonzalez-Ceron, L.; Gomez-Perez, D.J.; Santillan-Valenzuela, F.; Ovilla-Munoz, M.; Guzman-Bracho, C.; Pech-May, A.; Amores, G.R.; Montoya-Perez, A.; Villarreal-Trevino, C. Population Dynamics of *Plasmodium vivax* in Mexico Determined by CSP, Pvs25, and SSU 18S rRNA S-Type Polymorphism Analyses. *Microorganisms* **2025**, *13*, 2221. [CrossRef] [PubMed]
36. Chaves, L.F.; Huber, J.H.; Rojas Salas, O.; Ramirez Rojas, M.; Romero, L.M.; Gutierrez Alvarado, J.M.; Perkins, T.A.; Prado, M.; Rodriguez, R.M. Malaria Elimination in Costa Rica: Changes in Treatment and Mass Drug Administration. *Microorganisms* **2020**, *8*, 984. [CrossRef] [PubMed]

37. Labadie-Bracho, M.Y.; Adhin, M.R. Advocating for PCR-RFLP as molecular tool within malaria programs in low endemic areas and low resource settings. *PLoS Negl. Trop. Dis.* **2023**, *17*, e0011747. [CrossRef] [PubMed]
38. Escobar, D.; Archaga, O.; Reyes, A.; Palma, A.; Larson, R.T.; Vasquez, G.M.; Fontecha, G. A Follow-Up to the Geographical Distribution of *Anopheles* Species in Malaria-Endemic and Non-Endemic Areas of Honduras. *Insects* **2022**, *13*, 548. [CrossRef] [PubMed]

Disclaimer/Publisher's Note: The statements, opinions and data contained in all publications are solely those of the individual author(s) and contributor(s) and not of MDPI and/or the editor(s). MDPI and/or the editor(s) disclaim responsibility for any injury to people or property resulting from any ideas, methods, instructions or products referred to in the content.